This is the peer reviewed version of the following article: T. Chen, Q. Xue, K.-C. Leung, B. T. W. Lo, Recent Advances of Precise Cu Nanoclusters in Microporous Materials. Chem. Asian J. 2020, 15, 1819-1828, which has been published in final form at https://doi.org/10.1002/asia.202000331. This article may be used for non-commercial purposes in accordance with Wiley Terms and Conditions for Use of Self-Archived Versions.

Recent advances of precise Cu nanoclusters in microporous materials

Tianxiang Chen[a,b], Qi Xue[a,b], Kwan-Chee Leung[a,b], and Benedict T.W. Lo[a,b]*

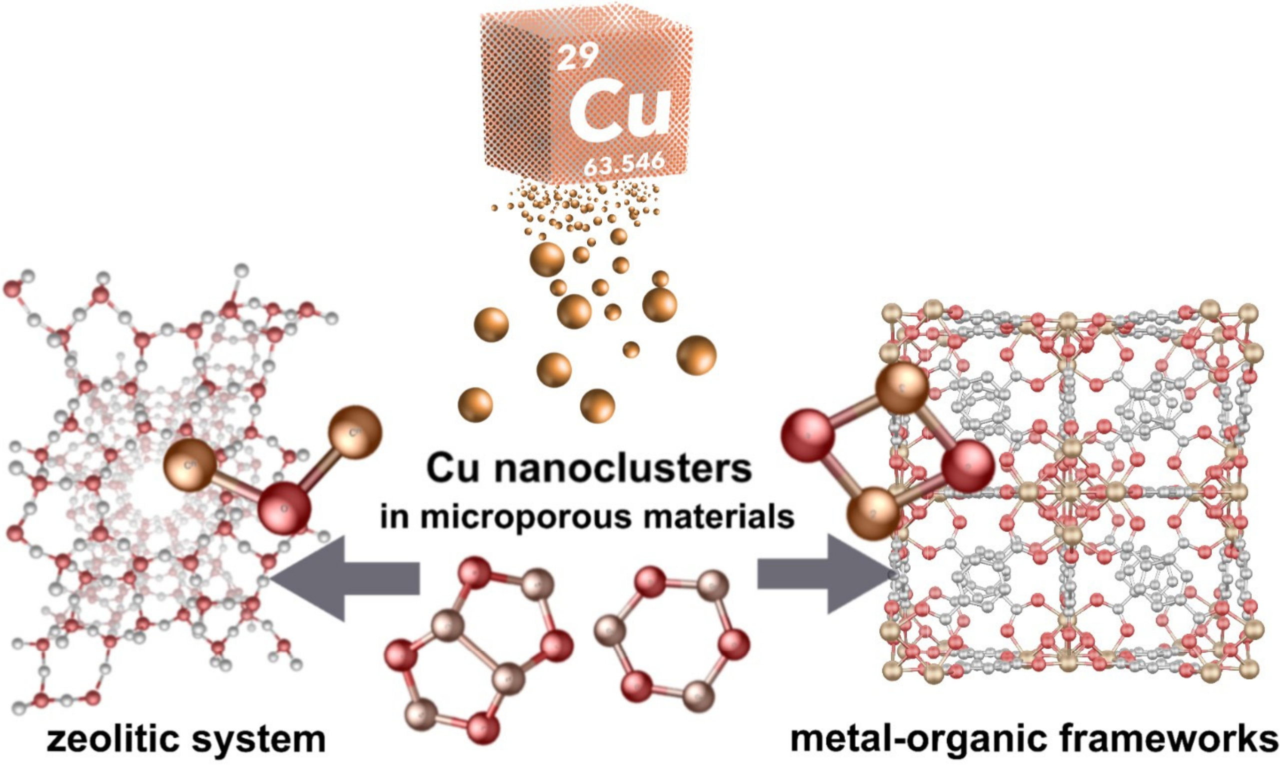

[a] T. Chen, Q. Xue, K.-C. Leung and B.T.W. Lo
State Key Laboratory of Chemical Biology and Drug Discovery
Department of Applied Biology and Chemical Technology
The Hong Kong Polytechnic University
Hong Kong SAR
E-mail: benedict.tw.lo@polyu.edu.hk
[b] T. Chen, Q. Xue, K.-C. Leung and B.T.W. Lo
The Hong Kong Polytechnic University Shenzhen Research Institute
Shenzhen Hi-tech Industrial Park
Shenzhen 518000
China

Abstract: This mini-review highlights some recent advances in the rational design of precise Cu nanoclusters supported on microporous materials, including zeolites and metal-organic frameworks. The development of comprehensive characterisation techniques enables scientists to elucidate the structure-activity relationship of these catalysts, which aids the subsequent engineering of more superior catalytic systems at an atomistic perspective.

1. Introduction

The current prominent era of nanoscience has led to an extensive boom of scientific and technological development. Nanomaterials are used extensively in society. Some notable examples include nano-TiO_2 in physical sunscreens[1], the homogeneous Ziegler–Natta catalyst for alkene polymerisation[2], and nano-CeO_2 for hydrogen production from CO and water feedstock[3,4]. In general, nanomaterials are classified by particles with a typical size distribution of less than 100 nm, where single atoms (SAs) are at the extreme end of the nanoscience spectrum. Nanomaterials have extremely interesting chemical and physical properties that are different from typical bulk materials. They bridge between bulk (classical chemistry) and atomic/molecular species (quantum chemistry), where the concept of discrete quantum levels in atomic/molecular structures can be fine-tuned based on the atomicity of the species. For instance, as reviewed by Liu and Corma, Au nanoparticles (NPs) illustrate notably variable work functions and electronic structures with discrete HOMO-LUMO separations, see Figure 1[5]. Based on the DFT calculations, for Au NPs > 2 nm, the energy levels gradually become continuous, that is consistent with the band theory.

Unlike the more mature characterisation of inorganic metal complexes, a reliable characterisation of supported SAs and well-defined nanoclusters (NCs) however could be difficultly achieved in the past due to technical limitations. It thus hindered the development of this class of highly potential solid-state materials. Thanks to the rapid technical advancement, these nanomaterials can be more extensively elucidated with higher clarity and reliability. Even single metal species can now be directly observed using suitable high-resolution electron microscopes[6,7]. By combining with other advanced scattering and spectroscopic techniques, the structural information of this new class of materials can be revealed at an atomistic resolution[8–10]. With the input of crucial structural information, researchers can more confidently design sub-nm materials with more precise atomicity.

The heterogeneous catalysis community has recently reported significant research progress by the rational design and the utilisation of these supported sub-nm NCs[11–13]. The connections between experimental findings in sub-nm materials with the predictions from quantum/classical mechanics are crucial to reveal fundamental chemistry which aids further optimisation. Not only the size (related to atomicity) of a NC matters but the morphology and coordination environments of the species also play a key role in the catalytic properties. We, to date, still cannot accurately predict the effect of these parameters on the catalysis of NCs materials.

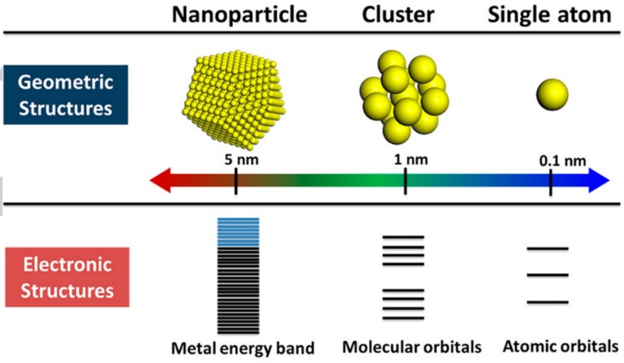

Figure 1. Geometric and electronic structures of SAs, NCs, and nanoparticles[5]. Reprinted with permission from Ref. 5. Copyright (2018) American Chemical Society.

Due to the high surface-area-to-volume ratio, bimetallic and trimetallic NCs are highly reactive and exhibit colloidal instability when compared to their bulk counterparts. They can be stabilised by different approaches, such as through ligand stabilisation[14–16], through supporting on transition-metal oxides[17,18], and through encapsulation within porous materials[19–22] (*e.g.* zeolites and metal-organic frameworks (MOFs)). Nature has been a great source of inspiration for many researchers, such as Schoonheydt *et al*. have fabricated O_2-activated Cu-ZSM-5 based on the Cu-core in the particulate form methane monooxygenase (pMMO) that can oxidise the C-H bond in methane for providing energy for bacterial metabolic activities[23]. Kiss *et al*. have designed imidazolate-bridged Cu/Zn bimetallic complex to mimic the Cu-Zn-core of superoxide that offers antioxidant defence in most of the living cells exposed to molecular oxygen[24].

The inorganic metal complex approach can undeniably deliver the precise synthesis and characterisation of SAs and NCs. Based on the rational design of different ligation systems, the local electronic and geometric structures of the metal cores can be finely tuned. There have been extensive works covering different perspectives of various synthesis and preparation of inorganic Cu complexes[14,25,26]. Typically, their crystal structures can be revealed using a combination of single-crystal X-ray diffraction[27–30] and nuclear magnetic resonance spectroscopy[31,32].

The use of heterogeneous catalysts, such as nanomaterials and porous materials, are beneficial to many industrial processes, thanks to the ease of catalyst-product separation and their high thermal/chemical stability. Crystalline and porous zeolites and MOFs can also be used to host SAs and NCs with well-defined structures to construct artificial metalloenzymatic systems (*cf.* zeozymes)[33–36]. Historically, zeolites were one of the first inorganic scaffolds that can stabilise SAs and NCs due to the framework confinement and unique framework functionalities.[37] The most studied catalysis applications are the selective oxidation of methane and the selective catalytic reduction (SCR) of NOx (as illustrated in Figure 2)[38]. As the authors are more experienced in the catalytic science of metal species over solid-state microporous materials, this mini-review will highlight the recent progress in the design of supported Cu NCs in zeolites and MOFs for catalytic applications.

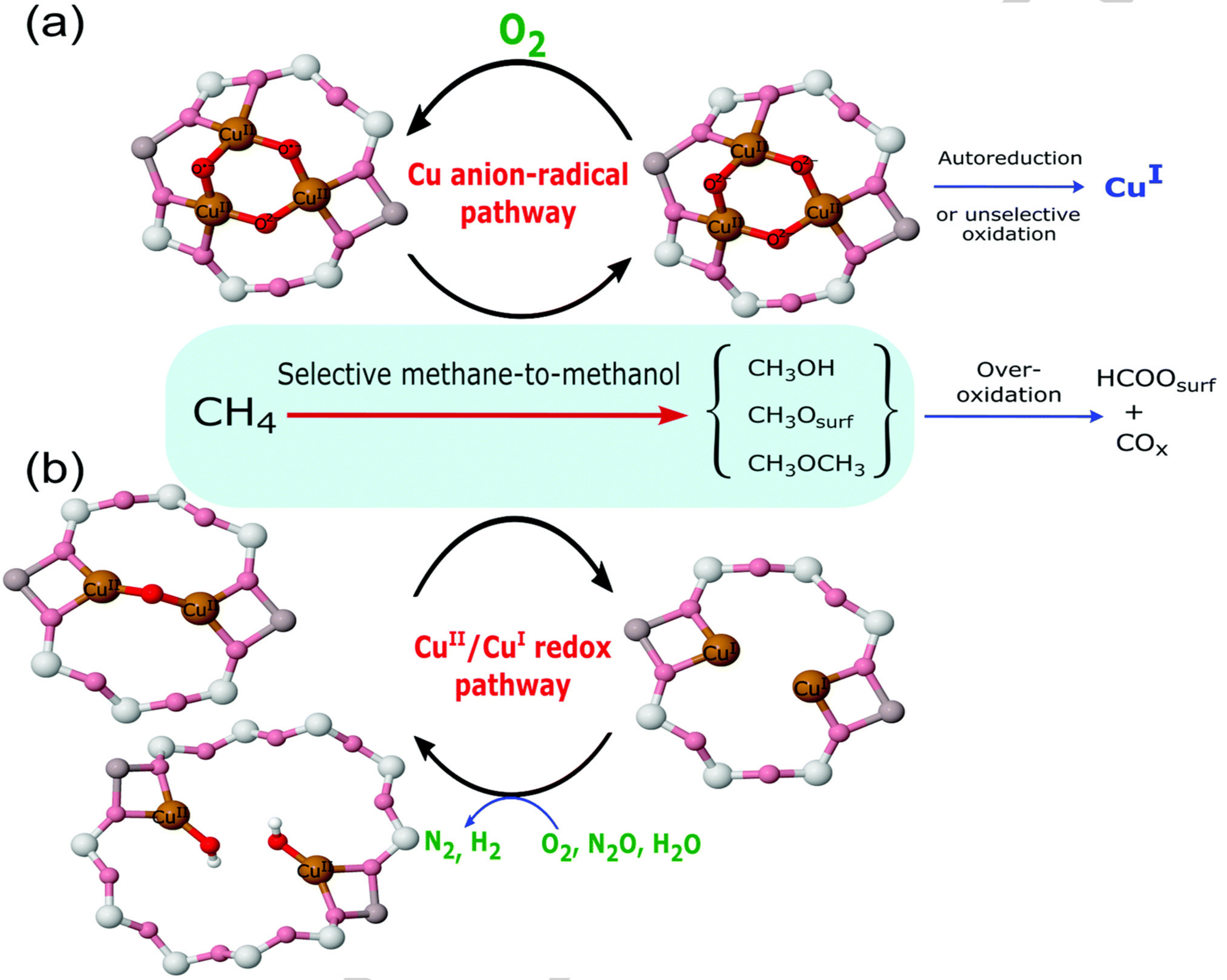

Figure 2. A schematic illustration of the two reaction pathways derived for the selective conversion of methane to methanol over Cu-containing zeolites: (a) the mechanism wherein the required electrons are handled via the formation of an oxyl radical species; (b) the mechanism localised at the copper centres with concurrent reduction of two Cu^{II} to two $Cu^{(I)}$[38]. Reproduced from Ref. 38 with permission from The Royal Society of Chemistry.

2. NCs in microporous materials

Inspired by the natural enzyme systems, many researchers have made substantial progress in mimicking the metal-containing cofactors of different natural metalloenzymes. The support and encapsulation approaches are realistic alternatives in offering extensive possibilities for the rational design and precise control of electronic and geometric structures for catalytic applications. Porous materials are widely used as the support to stabilise reactive metal sites, whereas the relatively inert framework can offer protein-like scaffold structures. Different approaches to synthesise artificial metalloenzymes have been investigated[39–43]. Among these systems, zeolites and MOFs are the most studied substrate. Although the selectivity or catalytic activity of these artificial metalloenzymes are generally still inferior to the natural enzymatic systems, their greater thermal and chemical stabilities have attracted the attention of many heterogeneous catalysis chemists.[44] NCs can exhibit different electronic and geometric structures by tuning the number of metal sites and coordination environments. These structures can be modified (*e.g.* to a proper valence state) to meet the needs of specific catalysis reactions.

2.1. Supported on zeolites

Aluminosilicate in origin, zeolites are a class of porous minerals that are used commonly as commercial adsorbents and catalysts. Since Axel Fredrik Cronstedt named ‘zeolites’ in 1756, zeolites with different framework structures have been continuously discovered and synthesised in the laboratory. More than 248 unique zeolite framework topologies have been identified as of April 2019[45]. Zeolites are microporous materials that possess pores (or channels) ranging from 2.8 Å (sodalite, ***SOD***) to 10.1 Å (ECR-34, ***ETR***), see Figure 3[46]. Besides the difference in the pore sizes, the pore shapes are also drastically different from each other. The adjustable pore structure and inherent Brønsted acidity (from charge compensation of Si^{IV} by Al^{III}) provide an excellent environment to stabilise Cu NCs.

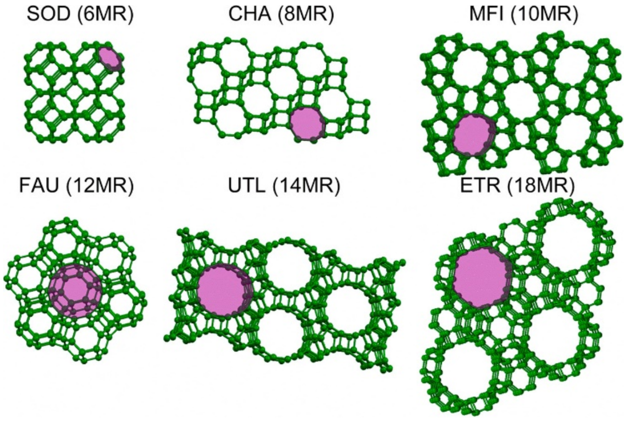

Figure 3. Zeolite topologies with different pore architectures: ***SOD*** with 6-membered ring (6-MR) pores of 2.8 Å; ***CHA*** (3.8 Å); ***MFI*** (~5.5 Å); ***FAU*** (7.4 Å); ***UTL*** (~9.5 Å); and ***ETR*** (10.1 Å)[46].

Due to the extensive use of zeolites in the chemical and petrochemical industries, researchers have devoted much effort in optimising the catalytic performance. In the early works, the direct incorporation of Cu (and other metals) species through ion-exchange and wet-impregnation into the zeolitic framework was common[47–49]. Multinuclear NCs can be formed upon thermal dehydration and reduction at high temperature[50,51]. Although we present an extensive collection of well-characterised Cu NCs encapsulated in zeolites, the synthesis of precisely controlled NCs remains challenging. In particular, as demonstrated in the catalysis of many inorganic Cu complexes where the electronic and geometric structures are stringent requirements, the lack of a well-controlled analogue in zeolites is a major shortcoming.

Zeolites with Cu incorporation have been a popular research area due to its potential to be effective catalysts for the selective oxidation of methane to methanol[52]. It is generally believed that the unique local environmental of Cu NCs within the constrained zeolitic frameworks can offer superior local and electronic structures to interact with methane, which may provide possible pathways for the subsequent selective oxidation of methane. The atomic and structural information, including the crystallographic location and coordination environment, of the Cu NCs in the zeolite frameworks are critical parameters for the catalytic performance.[41]

ZSM-5, Y and MOR are three common types of zeolites with relatively larger pore dimensions to host NCs for catalytic applications. These zeolites have distinct frameworks, with different channel dimensions and unique porous structures. Schoonheydt *et al.* used K- and Na-ZSM-5 as the host to anchor binuclear Cu NCs by over-ion-exchange with $Cu(CH_3COO)_2$[48]. Post-exchange drying at 383 K was applied to remove excess water from the pores. Extended X-ray absorption fine structure (EXAFS) spectroscopy, ultraviolet-visible spectroscopy (UV-Vis-NIR) and electron paramagnetic resonance (EPR) spectroscopy were combined to elucidate the active sites, bis(*μ*-oxo)bicopper(II) core $[Cu_2(\mu\text{-}O)_2]^{2+}$, within the ZSM-5 framework. The in situ EXAFS data has indicated the reversible formation and the reaction cycle between $Cu^+ \ldots Cu^+$ pair and $[Cu_2(\mu\text{-}O)_2]^{2+}$ during direct NO decomposition.

Solomon *et al.* investigated the same Cu-ZSM-5 catalyst for selective methane oxidation and identified the bent mono(μ-oxo)bicopper(II) species $[Cu_2O]^{2+}$ as the reaction immediate from the $[Cu_2(\mu\text{-}O)_2]^{2+}$ precursor using primarily resonance Raman spectroscopy (see Figure 4)[53]. The authors have employed oxygen-temperature-programmed desorption (O_2-TPD) measurements to provide extra insights into the conversion process between mono-*μ*-oxo and bis-*μ*-oxo species occurred upon heating. It has indicated the reversible O_2 capture/release function of the binuclear Cu core, which is akin to hemocyanin, the dioxygen carrier protein found in molluscs and anthropoids. Solomen *et al.* also combined resonance Raman spectroscopy with theoretical calculations to study the electronic structure of the bent $[Cu_2(\mu\text{-}O)]^{2+}$[54]. The polarisation of the low-lying singly-occupied molecular orbital of the $[Cu_2(\mu\text{-}O)]^{2+}$ core induces oxyl character to the bridging *μ*-O atom, which favours H atom abstraction from methane for selective oxidation to methanol.

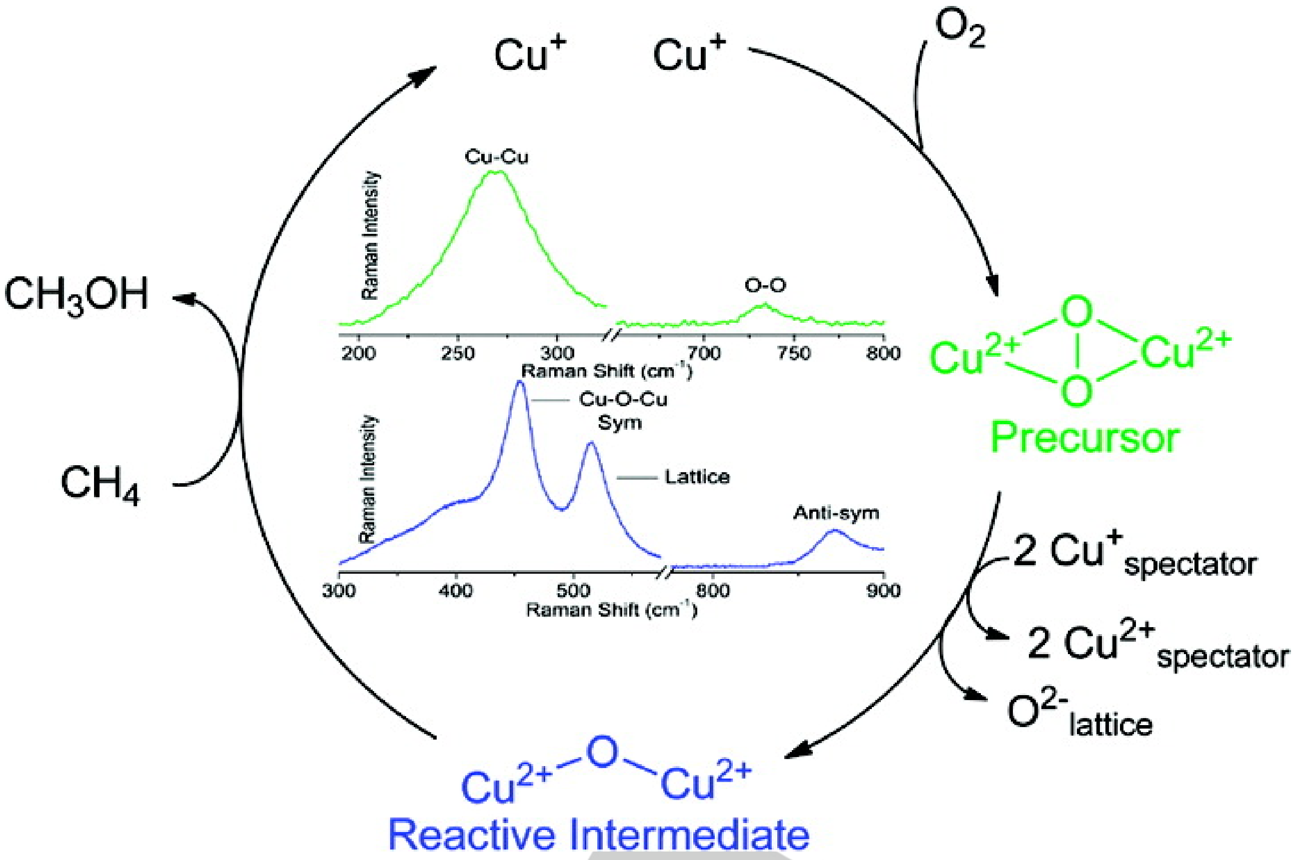

Figure 4. Proposed catalytic cycle for methane oxidation using Cu-ZSM-5. The resonance Raman spectra was present in the centre of figure[53]. Reprinted with permission from Ref. 53. Copyright (2010) American Chemical Society.

MOR zeolites are emerging supporting materials for Cu NCs due to the unique one-dimensional channel structure[41,55–59]. Schoonheydt *et al.* have also prepared binuclear Cu NCs in MOR using the over-ion-exchange method with $Cu(CH_3COO)_2$ at ambient temperature, followed by drying at 383 K[55,56]. Spectroscopic techniques, namely UV-Vis-NIR, EXAFS and EPR, were used to elucidate the structure of the $[Cu_2(\mu\text{-}O)_2]^{2+}$ in MOR, which was found with similar catalytic activity for the selective oxidation of methane (at 398 K) with the earlier mentioned $[Cu_2(\mu\text{-}O)_2]^{2+}$ in ZSM-5. In contrast, the $[Cu_2(\mu\text{-}O)_2]^{2+}$ in Y zeolites was found barely active for selective methane oxidation. The authors have proposed that the geometric factors of the Cu NCs cores are pivotal catalysis parameters, where the specific microporous structure of pentasil zeolites (in ZSM-5 and MOR) could be especially suited to stabilise $[Cu_2(\mu\text{-}O)_2]^{2+}$.

Besides binuclear Cu NCs, Lercher *et al.* have also stabilised trinuclear Cu-oxo NCs $[Cu_3(\mu\text{-}O)_3]^{2+}$ in MOR for the selective oxidation of methane to methanol[41]. The Cu_3-MOR samples were prepared by aqueous ion-exchange of H-MOR with $Cu(CH_3COO)_2$, followed by air drying at 383 K. Extra rinse cycles were performed to remove non-exchanged Cu ions that could form large CuO clusters upon the drying treatment. The authors combined EXAFS with density functional theory (DFT) calculations to determine the local single-site structure of the trinuclear Cu-oxo NCs and their interactions with the host MOR framework. As shown in Figure 5, $[Cu_3(\mu\text{-}O)_3]^{2+}$ is immobilised on two Al framework atoms on the 8-MR pore mouth of MOR. This example is another evidence that a unique geometric structure, such as the steric constraints of the NCs exerted by the rigid zeolitic frameworks, is a critical parameter to the catalytic activity, akin to the hydrophobic pore confinement in pMMO.

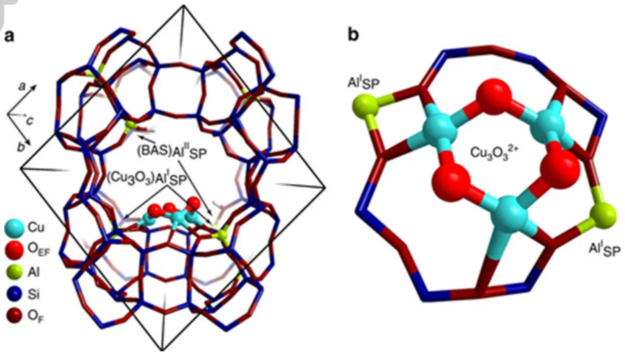

Figure 5. Structure and location of $[Cu_3(\mu\text{-}O)_3]^{2+}$ in MOR as predicted by combined EXAFS analysis and DFT calculations[41]. Reprinted with permission from Ref. 41. Copyright (2015), Springer Nature.

SSZ-13 and SAPO-34 adopt the ***CHA*** topology and have smaller pore dimensions that are constructed by 8-MR of T-O-T. Román-Leshkov *et al.* reported binuclear $[Cu–O–Cu]^{2+}$ NCs in SSZ-13 for selective partial methane oxidation at low temperature (see Figure 6)[60]. The dimeric Cu motif was prepared via proton-aided diffusion of hydrated Cu ions within the pores. It was determined as the primary active site. The formation of the dimeric motif can be maximised by using zeolites with high Al concentration. The residual zeolitic Brønsted acid sites (and water) can promote desorption of methanol from the dimeric Cu motif from further oxidation (to unwanted CO_2). A high concentration of Cu, however, can lead to aggregation forming NPs with larger particle size. This work has highlighted the significance of mechanistic information for the rational design of metal active sites and the optimisation of reaction conditions.

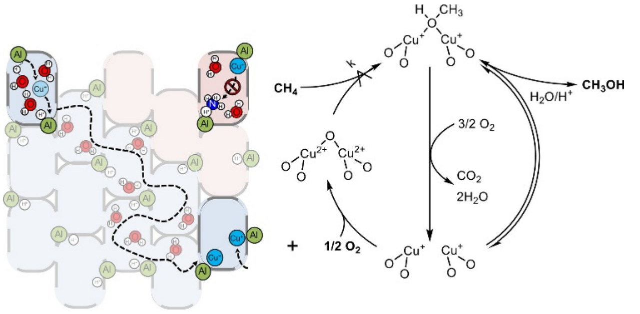

Figure 6. Depiction of hypothesised H^+/H_2O-aided diffusion of Cu^+ and NH_3 inhibition within SSZ-13 to form Cu dimers relevant to the proposed catalytic methane oxidation cycle. Single O atoms may correspond to framework zeolite O atoms or coordinating H_2O molecules[60]. Reprinted with permission from Ref. 60. Copyright (2019) American Chemical Society.

Operando XAS and DFT calculations have been used to study the structure-activity relationship on the productivity and Cu speciation during the key process steps in Cu-SSZ-13[61]. The $Z[Cu^{II}OH]$ complexes were determined as a key precursor, without direct involvement, for the formation of the active trimeric Cu motif for selective oxidation of methane at high temperature. A highly active superoxide site on CuO NCs encapsulated in SAPO-34 for the selective oxidation of ammonia at low temperature was reported by Chen *et al*.[62] As presented in Figure 7, it was synthesised through a multi-step 'Trojan Horse' approach: the first Cu sites were loaded in the one-pot synthesis during the hydrothermal process (to form isolated Cu sites), followed with additional Cu^{II} impregnation (to deposit bulk CuO). A subsequent activation process is needed to form confined CuO NCs from the two species. The structure of the CuO NCs has been characterised by combined XAS, in situ Raman and in situ DRIFT spectroscopy characterisation.

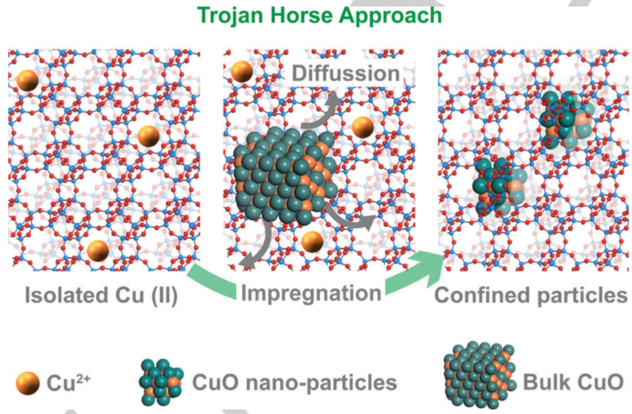

Figure 7. Schematic diagram for the preparation of CuO@SAPO-34 by the Trojan Horse approach[62]. Reprinted with permission from Ref. 62. Copyright (2019) American Chemical Society.

Besides microporous zeolites, mesoporous zeolites, with hierarchical structures and pore diameter > 2 nm, are also popular host to support Cu NCs. Wang *et al.* utilised γ-aminopropyl triethoxysilane to add amine basic site functionality (see Scheme 1)[63]. The amine sites were used to interact with incoming copper(II)acetylacetonate. The organic moieties were subsequently removed by air calcination. The authors evaluated the concentrations of the isolated Cu^{II} species and oligomeric CuO_x species using hydrogen-temperature-programmed reduction (H_2-TPR) and EPR spectroscopy. The in situ formation of Cu^I, from the reduction of the isolated Cu^{II} species, has been found responsible for the activation of incoming O_2 for the partial oxidation of methane to formaldehyde.

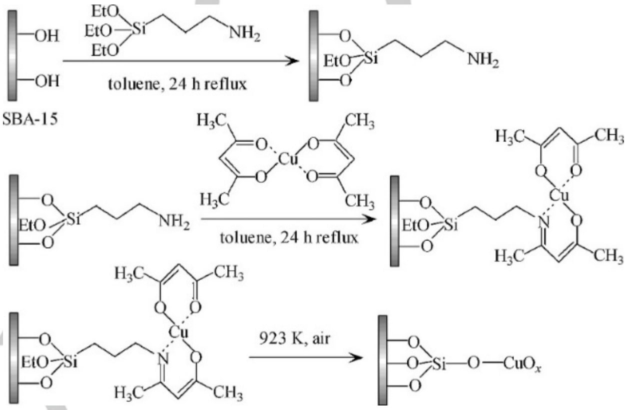

Scheme 1. Preparation of CuOx/SBA-15 catalysts by the grafting method[63]. Reprinted from Ref. 63, with permission from Elsevier.

2.2 Over metal-organic framework (MOF) systems

Metal-organic frameworks (MOFs) materials are an assembly of metal ions and organic molecules that combine to form coordinated and crystalline solids. The nodes are either metal ions or multinuclear metal-core clusters, whereas the linkers are multi-basic organic molecules. MOFs have captured wide interest in various applications, such as gas separation, proton conductivity, biomedicine and catalysis. Unlike the zeolitic counterpart, MOFs also exhibit high potential in photocatalysis thanks to their intrinsic crystalline nature, structural diversity, tuneable frameworks and adjustable electronic structures. MOFs are considered as an array of self-assembled molecular catalysts rather than conventional semiconductors.[64] Besides the fabrication of MOFs with multinuclear Cu metal node, the MOF framework can be chemically functionalised that has offered great potential in the decoration of extra-framework species through different approaches.

2.2.1 Framework Cu species in MOFs

The fabrication of MOFs relies heavily on the coordination interactions between Lewis acidic metal ions or metal-core clusters and Lewis basic organic ligands. Various organic linker molecules were specifically designed that led to the engineering of different MOF structures. The framework can be chemically functionalised. In one of the earliest reports, the crystalline structure of HKUST-1 MOF, as confirmed by PXRD, contains a binuclear Cu_2-core as the node and 1,3,5-benzenetricarboxylic acid (BTC) as the linker[65]. HKUST-1 has interconnected

$[Cu_2(O_2CR)_4]$ units (where R is an aromatic ring), which create a three-dimensional channel system with a pore size of 1 nm and an accessible porosity of about 40% in the solid. Williams *et al*. have further replaced the di-axial water ligands in HKUST-1 by two pyridine molecules, where the framework is stable up to 240 °C[65]. Other MOFs that contain binuclear Cu_2-core have also been reported, such as $Cu_2(EBTC)(H_2O)_2{\cdot}[G]$ ($EBTC^{4-}$ = 1,1′-ethynebenzene-3,3′,5,5′-tetracarboxylate; G = guest molecules and represent DMF, DMSO and H_2O)[66], and MOF-505[67]. MOF-505 is constructed by 3,3’,5,5’-biphenyltetracarboxylic acid as the linker and a binuclear Cu_2-core as the node. Similar to other MOF materials, the MOF-505 can only be crystallised in the additional presence of an organic solvent, where MOF-505 is stabilised by water and dimethylformamide (DMF).

Tetranuclear Cu_4- and octanuclear Cu_8-core MOFs have also been reported, such as highly proton conducting $Cu_4(\mu_3\text{-}OH)_2$-based MOF that possesses large hydrophilic channels (see Figure 8)[40], $Cu_4(OH)_2(CO_2)_4(SO_3)_2$-based MOF that possesses one-dimensional irregular channels[43], a $Cu_4(OH)_2$-based MOF constructed using a flexible tripodal ligand (tri(2-carboxyethyl)-isocyanurate) showing intracluster dominant antiferromagnetic interactions[68], and a MOF with octanuclear copper cluster secondary building units using 3-connected 4-(pyrimidin-5-yl) benzoic acid (4-PmBC) as the ligands[69].

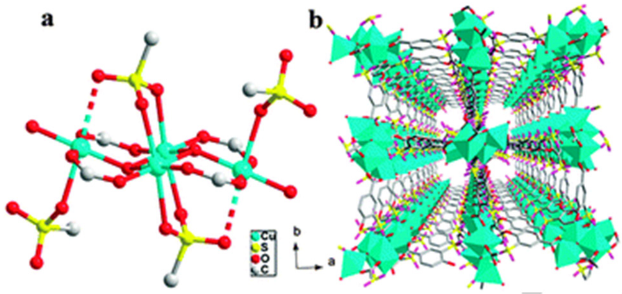

Figure 8. (a) A view of a tetrameric Cu_4 NC. (b) Central projection of the MOF viewed down the c-axis. The solvent water molecules and hydrogen atoms are omitted for clarity[40]. Reproduced from Ref. 40 with permission from The Royal Society of Chemistry.

Recently, Wang *et al.* firstly reported a rigid copper thiolate cluster-assembled material (Cu_{12}bpy, bpy = 4,4′-bipyridine).[74] They demonstrated an increase in the content of dense copper of copper azide composites, which contributed to the high output energy of copper azide-based explosives.

In addition to MOFs with multinuclear Cu_n-core units, there are various examples possess CuI-based nodes. Boilet *et al*. reported a Cu_4I_4-based MOF that has a classical cubane nodal cluster formed by four Cu atoms and four I atoms which alternatively occupy the corners of a distorted cube[71]. A related MOF has been constructed by a Cu_4I_4-siloxanol-functionalised luminescent cluster[72]. Lu *et al*. reported a Cu_6I_4-based three-dimensional MOF that has a (4,8)-connected fluorite topological network[42]. Strong yellow light emission was observed from the photoluminescent measurements. A cationic two-dimensional MOF consisting a cationic $[Cu_6I_5]^+$ cluster and two neutral ligand motif was reported by Boomishankar *et al.*[73] Unusual thermochromic behaviour was observed, the two-dimensional MOF emitting a blue fluorescence at 298 K due to the 3-quinolinyl chromophore and an orange-yellow phosphorescence at 77 K from the $[Cu_6I_5]^+$ unit.

2.2.2 Extra-framework Cu species in MOFs

MOFs are regarded as an excellent host to support extra-framework metal species thanks to the porous property and intrinsic framework functionalities. Besides the presence of nodal Cu-core in MOFs, specific framework functionalities can also be utilised to incorporate or encapsulate extra-framework Cu species[74]. Chapman *et al*. have functionalised NU-1000 (a Zr-based MOF) with Cu through atomic layer deposition[75]. The local structure of the supported Cu species was probed by combining pair distribution function analysis and difference envelope density analysis of the in situ synchrotron-based X-ray scattering data (see Figure 9). The distribution of the Cu species within NU-1000 and the distortions of the NU-1000 lattice under conditions relevant to catalysis were revealed. Cu-*oxo* clusters were formed within the small pores that connect the triangular and hexagonal channels.

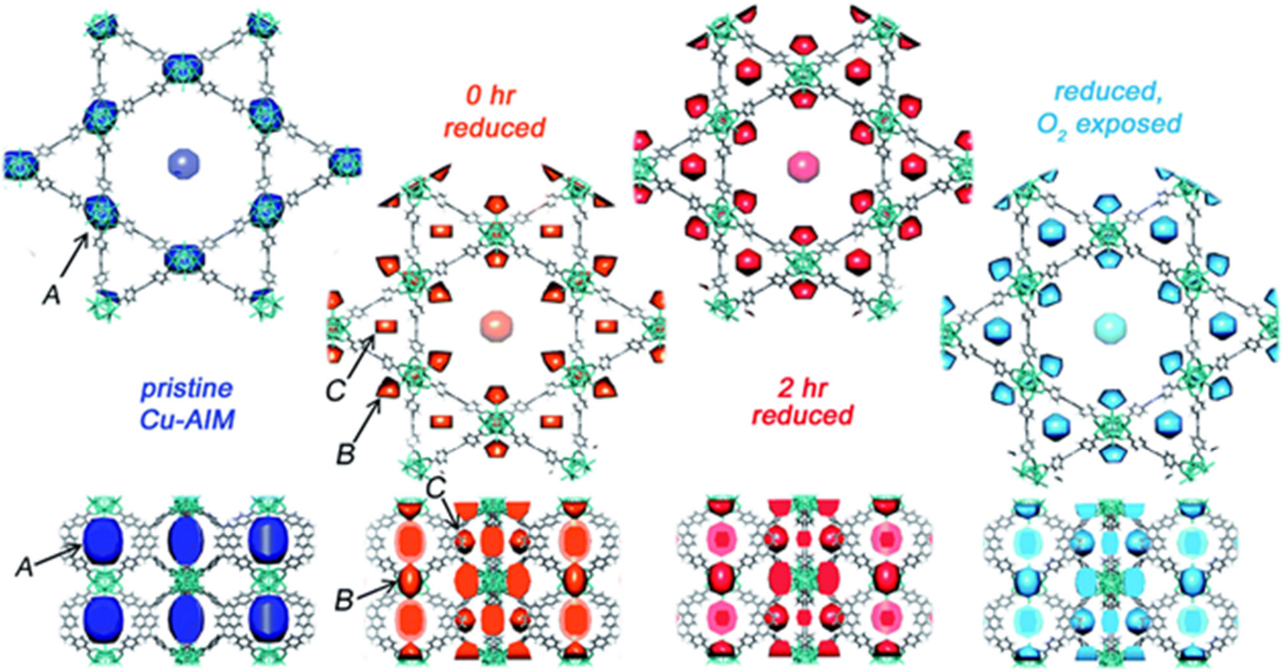

Figure 9. Difference envelope density maps viewed parallel (top) and perpendicular (bottom) to the *c*-axis for Cu-AIM in the pristine state, at the beginning and end of reduction at 200 °C and following re-oxidation[75]. Reproduced from Ref. 75 with permission from The Royal Society of Chemistry.

As far as we are aware, the defect sites and Lewis basic moieties of various MOF structures have also been utilised to anchor Cu species. Notably, Yaghi *et al*. have fabricated highly active and stable Cu SAs that form covalent attachment onto the intrinsic defects of the Zr_6O_4 node of UiO-66 (a Zr-based MOF, see Figure 10)[76]. Electrostatic interactions originated by the -SO_3H moieties of MIL-101-SO_3H (a Cr-based MOF) has been applied to capture Cu^{2+} through ion-exchange[77]. The anionic sulfonate groups provide facile handles to immobilise open metal cations through charge-assisted coordination. Despite there are only reports over extra-framework Cu SAs encapsulated by MOFs, it is anticipated that extensive research of Cu NCs in MOFs will be developed via post-synthetic modification of the host framework.

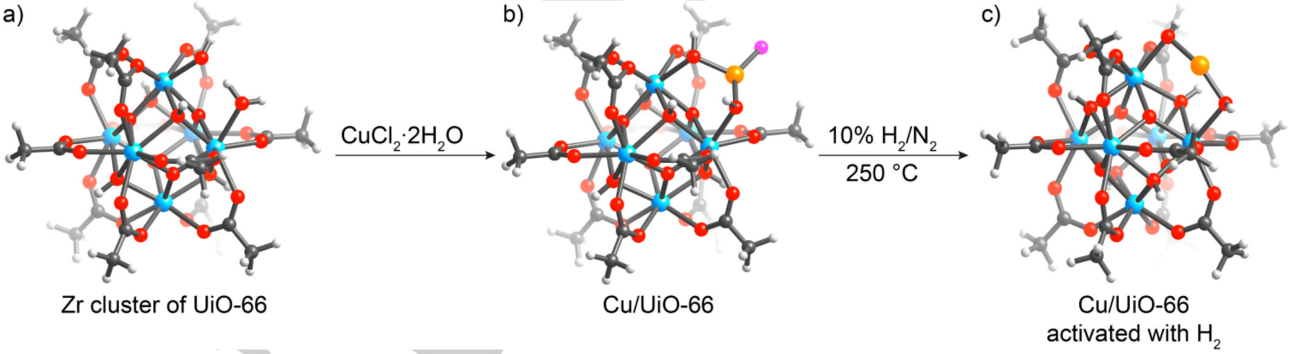

Zr cluster of UiO-66

Cu/UiO-66

Cu/UiO-66
activated with H_2

Figure 10. DFT calculated structures (a) of defective UiO-66, (b) of a Cu/UiO-66 catalyst where Cu is coordinated to a −OH/–OH2 defect site of UiO-66, and (c) of a Cu/UiO-66 catalyst after activation with H_2. Atom labelling: C = black; O = red; Cl = pink; Cu = orange; Zr = blue; H = light grey[76]. Reprinted with permission from Ref. 76. Copyright (2019) American Chemical Society.

3. Conclusion and perspective

Catalytic systems utilising Cu NCs supported on zeolitic and MOF materials are emerging in recent years. One of the most attractive catalytic applications is the selective oxidation of methane to methanol for the sustainable provision of fuel and commodity chemicals. Thanks to the tuneable functionality of zeolitic and MOF framework scaffolds, the highly crystalline hierarchical structures can readily immobilise intrinsically unstable metal NCs. The electronic and geometric structures of the NCs are critical parameters for catalysis. Various recent findings have revealed the structure-activity relationships of Cu NCs, such as oligomeric CuO_x species, CuO species, Z[Cu^{II}OH], $[Cu_2O]^{2+}$, $[Cu_2(\mu\text{-}O)_2]^{2+}$,

$[Cu_2(\mu\text{-}O)]^{2+}$, $[Cu\text{–}O\text{–}Cu]^{2+}$ and $[Cu_3(\mu\text{-}O)_3]^{2+}$, with respect to the catalytic performance.

It is increasingly accepted that a single technique can insufficiently determine the catalytic science associated with respect to the structures of the encapsulated and ultra-fine active sites within zeolitic and MOF materials. As reviewed in this article, most recent research reports have employed multiple characterisation techniques that include crystallographic, spectroscopic and computational approaches. Whereas the diffraction-based crystallographic techniques can be used to derive the atomic and structural parameters of the supported NCs, spectroscopic techniques, such as UV-Vis-NIR, FTIR and XAS, can be used to reveal the respective coordination and bonding information. The experimental data generated can be further verified with theoretical calculations to provide an extensive investigation of the entire catalytic system. The structural elucidation, hence, offers a sensible guide for the future design of related supported catalytic systems. Not only these mentioned characterisation techniques can be combined to provide a comprehensive understanding of the catalysis chemistry, but more superior and optimised catalytic systems can also be consequently achieved.

Acknowledgements

We thank the Hong Kong Research Grants Council (PolyU 253009/18P) and the National Natural Science Foundation of China (21902139) for financial support.

Keywords: Cu Nanoclusters • Zeolites • Metal-organic frameworks (MOFs) • Catalysis

[1] G. J. Nohynek, J. Lademann, C. Ribaud, M. S. Roberts, *Crit. Rev. Toxicol.* **2007**, *37*, 251–277.
[2] K. Endo, R. Ueda, T. Otsu, *Polym. J.* **1991**, *23*, 1173–1178.
[3] Q. Fu, A. Weber, M. Flytzani-Stephanopoulos, *Catal. Letters* **2001**, *77*, 87–95.
[4] Z. Y. Yuan, V. Idakiev, A. Vantomme, T. Tabakova, T. Z. Ren, B. L. Su, *Catal. Today* **2008**, *131*, 203–210.
[5] L. Liu, A. Corma, *Chem. Rev.* **2018**, *118*, 4981–5079.
[6] J. Jones, H. Xiong, A. T. DeLaRiva, E. J. Peterson, H. Pham, S. R. Challa, G. Qi, S. Oh, M. H. Wiebenga, X. I. P. Hernández, Y. Wang, A. K. Datye, *Science (80-.).* **2016**, *353*, 150–154.
[7] V. Ortalan, A. Uzun, B. C. Gates, N. D. Browning, *Nat. Nanotechnol.* **2010**, *5*, 506–510.
[8] B. Qiao, A. Wang, X. Yang, L. F. Allard, Z. Jiang, Y. Cui, J. Liu, J. Li, T. Zhang, *Nat. Chem.* **2011**, *3*, 634–641.
[9] M. Moses-Debusk, M. Yoon, L. F. Allard, D. R. Mullins, Z. Wu, X. Yang, G. Veith, G. M. Stocks, C. K. Narula, *J. Am. Chem. Soc.* **2013**, *135*, 12634–12645.
[10] J. Gu, C. S. Hsu, L. Bai, H. M. Chen, X. Hu, *Science (80-.).* **2019**, *364*, 1091–1094.
[11] E. Fernández, M. A. Rivero-Crespo, I. Domínguez, P. Rubio-Marqués, J. Oliver-Meseguer, L. Liu, M. Cabrero-Antonino, R. Gavara, J. C. Hernández-Garrido, M. Boronat, A. Leyva-Pérez, A. Corma, *J. Am. Chem. Soc.* **2019**, *141*, 1928–1940.
[12] T.-N. Ye, Z. Xiao, J. Li, Y. Gong, H. Abe, Y. Niwa, M. Sasase, M. Kitano, H. Hosono, *Nat. Commun.* **2020**, *11*, 1020.
[13] L. Liu, M. Lopez-Haro, C. W. Lopes, C. Li, P. Concepcion, L. Simonelli, J. J. Calvino, A. Corma, *Nat. Mater.* **2019**, *18*, 866–873.
[14] R. Cao, P. Müller, S. J. Lippard, *J. Am. Chem. Soc.* **2010**, *132*, 17366–17369.
[15] S. I. Chan, Y. J. Lu, P. Nagababu, S. Maji, M. C. Hung, M. M. Lee, I. J. Hsu, P. D. Minh, J. C. H. Lai, K. Y. Ng, S. Ramalingam, S. S. F. Yu, M. K. Chan, *Angew. Chemie - Int. Ed.* **2013**, *52*, 3731–3735.
[16] T. Zhang, C. Wang, S. Liu, J. L. Wang, W. Lin, *J. Am. Chem. Soc.* **2014**, *136*, 273–281.
[17] A. A. Herzing, C. J. Kiely, A. F. Carley, P. Landon, G. J. Hutchings, *Science (80-.).* **2008**, *321*, 1331–1335.
[18] H. Xu, C. Q. Xu, D. Cheng, J. Li, *Catal. Sci. Technol.* **2017**, *7*, 5860–5871.
[19] M. Yang, S. Li, Y. Wang, J. A. Herron, Y. Xu, L. F. Allard, S. Lee, J. Huang, M. Mavrikakis, M. Flytzani-Stephanopoulos, *Science (80-.).* **2014**, *346*, 1498–1501.
[20] J. Shan, M. Li, L. F. Allard, S. Lee, M. Flytzani-Stephanopoulos, *Nature* **2017**, *551*, 605–608.
[21] K. I. Otake, Y. Cui, C. T. Buru, Z. Li, J. T. Hupp, O. K. Farha, *J. Am. Chem. Soc.* **2018**, *140*, 8652–8656.
[22] X. Fang, Q. Shang, Y. Wang, L. Jiao, T. Yao, Y. Li, Q. Zhang, Y. Luo, H. L. Jiang, *Adv. Mater.* **2018**, *30*, 1705112.
[23] R. A. Himes, K. D. Karlin, *Curr. Opin. Chem. Biol.* **2009**, *13*, 119–131.
[24] I. Szilágyi, L. Horváth, I. Labádi, K. Hernadi, I. Pálinkó, T. Kiss, *Cent. Eur. J. Chem.* **2006**, *4*, 118–134.
[25] P. Nagababu, S. S. F. Yu, S. Maji, R. Ramu, S. I. Chan, *Catal. Sci. Technol.* **2014**, *4*, 930–935.
[26] S. Maji, J. C. M. Lee, Y. J. Lu, C. L. Chen, M. C. Hung, P. P. Y. Chen, S. S. F. Yu, S. I. Chan, *Chem. - A Eur. J.* **2012**, *18*, 3955–3968.
[27] Y. Funahashi, T. Nishikawa, Y. Wasada-Tsutsui, Y. Kajita, S. Yamaguchi, H. Arii, T. Ozawa, K. Jitsukawa, T. Tosha, S. Hirota, T. Kitagawa, H. Masuda, *J. Am. Chem. Soc.* **2008**, *130*, 16444–16445.
[28] A. Neuba, U. Flörke, W. Meyer-Klaucke, M. Salomone-Stagni, E. Bill, E. Bothe, P. Höfer, G. Henkel, *Angew. Chemie - Int. Ed.* **2011**, *50*, 4503–4507.
[29] M. Komiyama, S. Kina, K. Matsumura, J. Sumaoka, S. Tobey, V. M. Lynch, E. Anslyn, *J. Am. Chem. Soc.* **2002**, *124*, 13731–13736.
[30] H. Fu, Y. H. Zhou, W. L. Chen, Z. G. Deqing, M. L. Tong, L. N. Ji, Z. W. Mao, *J. Am. Chem. Soc.* **2006**, *128*, 4924–4925.
[31] A. Dijksman, I. W. C. E. Arends, R. A. Sheldon, *Org. Biomol. Chem.* **2003**, *1*, 3232–3237.
[32] K. S. Banu, T. Chattopadhyay, A. Banerjee, S. Bhattacharya, E. Suresh, M. Nethaji, E. Zangrando, D. Das, *Inorg. Chem.* **2008**, *47*, 7083–7093.
[33] F. Li, D. Hu, Y. Yuan, B. Luo, Y. Song, S. Xiao, G. Chen, Y. Fang, F. Lu, *Mol. Catal.* **2018**, *452*, 75–82.
[34] L. Liu, U. Díaz, R. Arenal, G. Agostini, P. Concepción, A. Corma, *Nat. Mater.* **2017**, *16*, 132–138.
[35] J. R. Bour, A. M. Wright, X. He, M. Dincă, *Chem. Sci.* **2020**, *11*, 1728–1737.
[36] J. Chen, L. Huang, Q. Wang, W. Wu, H. Zhang, Y. Fang, S. Dong, *Nanoscale* **2019**, *11*, 5960–5966.
[37] R. Gounder, E. Iglesia, *Chem. Commun.* **2013**, *49*, 3491–3509.
[38] M. A. Newton, A. J. Knorpp, V. L. Sushkevich, D. Palagin, J. A. van Bokhoven, *Chem. Soc. Rev.* **2020** DOI 10.1039/c7cs00709d.
[39] W. Zang, T. Yang, H. Zou, S. Xi, H. Zhang, X. Liu, Z. Kou, Y. Du, Y. P. Feng, L. Shen, L. Duan, J. Wang, S. J. Pennycook, *ACS Catal.* **2019**, *9*, 10166–10173.
[40] X. Y. Dong, R. Wang, J. Bin Li, S. Q. Zang, H. W. Hou, T. C. W. Mak, *Chem. Commun.* **2013**, *49*, 10590–10592.
[41] S. Grundner, M. A. C. Markovits, G. Li, M. Tromp, E. A. Pidko, E. J. M. Hensen, A. Jentys, M. Sanchez-Sanchez, J. A. Lercher, *Nat. Commun.* **2015**, *6*, 1–9.
[42] F. Wang, R. M. Yu, X. Y. Wu, C. Z. Lu, *Inorg. Chem. Commun.* **2012**, *19*, 70–72.
[43] X. Meng, S. Y. Song, X. Z. Song, M. Zhu, S. N. Zhao, L. L. Wu, H. J. Zhang, *Chem. Commun.* **2015**, *51*, 8150–8152.
[44] C. H. Lee, T. S. Lin, C. Y. Mou, *Nano Today* **2009**, *4*, 165–179.
[45] C. Baerlocher, L. B. McCusker, "Database of Zeolite Structures," **2014**.
[46] N. Kosinov, C. Liu, E. J. M. Hensen, E. A. Pidko, *Chem. Mater.* **2018**, *30*, 3177–3198.
[47] S. A. Yashnik, Z. R. Ismagilov, V. F. Anufrienko, *Catal. Today* **2005**, *110*, 310–322.
[48] M. H. Groothaert, J. A. Van Bokhoven, A. A. Battiston, B. M. Weckhuysen, R. A. Schoonheydt, *J. Am. Chem. Soc.* **2003**, *125*, 7629–7640.
[49] K. Hadjiivanov, H. Knözinger, *J. Catal.* **2000**, *191*, 480–485.
[50] L. Rodriguez-Santiago, M. Sierka, V. Branchadell, M. Sodupe, J. Sauer, *J. Am. Chem. Soc.* **1998**, *120*, 1545–1551.
[51] B. F. Mentzen, G. Bergeret, *J. Phys. Chem. C* **2007**, *111*, 12512–12516.
[52] P. Tomkins, M. Ranocchiari, J. A. Van Bokhoven, *Acc. Chem. Res.* **2017**, *50*, 418–425.
[53] P. J. Smeets, R. G. Hadt, J. S. Woertink, P. Vanelderen, R. A. Schoonheydt, B. F. Sels, E. I. Solomon, *J. Am. Chem. Soc.* **2010**, *132*, 14736–14738.
[54] J. S. Woertink, P. J. Smeets, M. H. Groothaert, M. A. Vance, B. F. Sels, R. A. Schoonheydt, E. I. Solomon, *Proc. Natl. Acad. Sci. U. S. A.* **2009**, *106*, 18908–18913.
[55] M. H. Groothaert, P. J. Smeets, B. F. Sels, P. A. Jacobs, R. A. Schoonheydt, *J. Am. Chem. Soc.* **2005**, *127*, 1394–1395.
[56] P. J. Smeets, M. H. Groothaert, R. A. Schoonheydt, *Catal. Today* **2005**, *110*, 303–309.

[57] A. R. Kulkarni, Z. J. Zhao, S. Siahrostami, J. K. Nørskov, F. Studt, *ACS Catal.* **2016**, *6*, 6531–6536.

[58] V. L. Sushkevich, D. Palagin, J. A. van Bokhoven, *Angew. Chemie - Int. Ed.* **2018**, *57*, 8906–8910.

[59] D. Palagin, A. J. Knorpp, A. B. Pinar, M. Ranocchiari, J. A. Van Bokhoven, *Nanoscale* **2017**, *9*, 1144–1153.

[60] K. T. Dinh, M. M. Sullivan, K. Narsimhan, P. Serna, R. J. Meyer, M. Dincă, Y. Román-Leshkov, *J. Am. Chem. Soc.* **2019**, *141*, 11641–11650.

[61] D. K. Pappas, E. Borfecchia, M. Dyballa, I. A. Pankin, K. A. Lomachenko, A. Martini, M. Signorile, S. Teketel, B. Arstad, G. Berlier, C. Lamberti, S. Bordiga, U. Olsbye, K. P. Lillerud, S. Svelle, P. Beato, *J. Am. Chem. Soc.* **2017**, *139*, 14961–14975.

[62] F. Han, M. Yuan, S. Mine, H. Sun, H. Chen, T. Toyao, M. Matsuoka, K. Zhu, J. Zhang, W. Wang, T. Xue, *ACS Catal.* **2019**, *9*, 10398–10408.

[63] D. An, Q. Zhang, Y. Wang, *Catal. Today* **2010**, *157*, 143–148.

[64] M. A. Nasalevich, M. Van Der Veen, F. Kapteijn, J. Gascon, *CrystEngComm* **2014**, *16*, 4919–4926.

[65] S. S. Y. Chui, S. M. F. Lo, J. P. H. Charmant, A. G. Orpen, I. D. Williams, *Science (80-.).* **1999**, *283*, 1148–1150.

[66] P. C. Guo, T. Y. Chen, X. M. Ren, C. Xiao, W. Jin, *Dalt. Trans.* **2014**, *43*, 6720–6727.

[67] B. Chen, N. W. Ockwig, A. R. Millward, D. S. Contreras, O. M. Yaghi, *Angew. Chemie - Int. Ed.* **2005**, *44*, 4745–4749.

[68] C. Hou, Y. L. Bai, X. L. Bao, L. Xu, R. G. Lin, S. Zhu, J. Fang, J. Xu, *Dalt. Trans.* **2015**, *44*, 7770–7773.

[69] J. Luo, J. Wang, G. Li, Q. Huo, Y. Liu, *Chem. Commun.* **2013**, *49*, 11433–11435.

[70] Q.-Y. Wang, L. Zhang, W.-M. He, L. Yang, C. Zhang, Z.-Y. Wang, R. Zhang, J.-H. Chen, S. Wang, S.-Q. Zang, T. C. W. Mak, *Chem. Eng. J.* **2020**, *389*, 124455.

[71] S. Perruchas, X. F. L. Goff, S. Maron, I. Maurin, F. Guillen, A. Garcia, T. Gacoin, J. P. Boilot, *J. Am. Chem. Soc.* **2010**, *132*, 10967–10969.

[72] S. Perruchas, N. Desboeufs, S. Maron, X. F. Le Goff, A. Fargues, A. Garcia, T. Gacoin, J. P. Boilot, *Inorg. Chem.* **2012**, *51*, 794–798.

[73] A. Yadav, A. K. Srivastava, A. Balamurugan, R. Boomishankar, *Dalt. Trans.* **2014**, *43*, 8166–8169.

[74] S. I. Vasylevskyy, G. A. Senchyk, A. B. Lysenko, E. B. Rusanov, A. N. Chernega, J. Jezierska, H. Krautscheid, K. V. Domasevitch, A. Ozarowski, *Inorg. Chem.* **2014**, *53*, 3642–3654.

[75] X. Y. Dong, R. Wang, J. Bin Li, S. Q. Zang, H. W. Hou, T. C. W. Mak, *Chem. Commun.* **2013**, *49*, 10590–10592.

[76] A. M. Abdel-Mageed, B. Rungtaweevoranit, M. Parlinska-Wojtan, X. Pei, O. M. Yaghi, R. Jürgen Behm, *J. Am. Chem. Soc.* **2019**, *141*, 5201–5210.

[77] W. J. Sun, E. Q. Gao, *Appl. Catal. A Gen.* **2019**, *569*, 110–116.

Chen is currently a PhD student working under the supervisor of Dr Benedict Tsz-woon Lo in The Hong Kong Polytechnic University in Hong Kong (China). He obtained his B.S. from Guangxi University in 2015 and M.S. from South China University of Technology in 2018. His research interest work is on the precise synthesis metal nanoclusters within zeolitic materials.

Xue obtained his B.Eng. from Jinan University (2014) and M.S. from China University of Petroleum (East China) (2018). Now he is a PhD student in The Hong Kong Polytechnic University (China) under the supervisor of Dr Benedict Tsz-woon Lo. His research interest work is on the single atom materials within metal-organic frameworks.

Leung was a research assistant in Lo's group and is currently a DPhil student at the University of Oxford (UK). He obtained his BSc from the University of Hong Kong and MSc from University College London. His research interest work is on porous materials and their catalytic applications.

Lo is a solid-state chemist who has interest in the fundamental aspects of microporous materials and their catalytic applications. He obtained his MChem and DPhil degrees from the St. John's College, the University of Oxford (UK). Since 2017, he has been a Research Assistant Professor at the Hong Kong Polytechnic University.

Entry for the Table of Contents

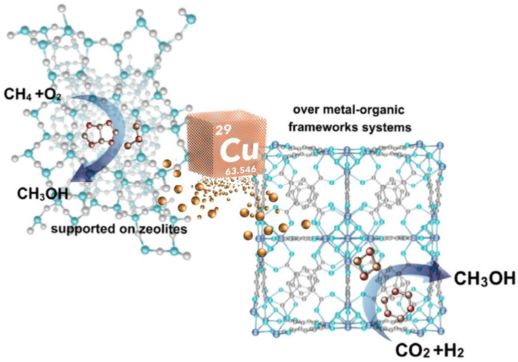

The synthesis of well-defined Cu nanoclusters within microporous materials is an emerging research area due to the high potential in the selective catalytic oxidation of methane to methanol. This mini-review highlights some recent advances in the fabrication of precise Cu nanoclusters supported on zeolites and metal-organic frameworks and their corresponding catalytic applications.